ISSN 0030-400X, Optics and Spectroscopy, 2017, Vol. 122, No. 6, pp. 859–871. © Pleiades Publishing, Ltd., 2017.
Original Russian Text © M.R. Cherkasov, 2017, published in Optika i Spektroskopiya, 2017, Vol. 122, No. 6, pp. 892–905.

SPECTROSCOPY OF ATOMS AND MOLECULES

# Broadening and Collisional Interference of Lines in the IR Spectra of Ammonia: Self-Broadening in the $\nu_1$ Band

**M. R. Cherkasov***

*National Research Tomsk Polytechnic University, Tomsk, 634050 Russia*
*Yurga Institute of Technology, Branch of the National Research Tomsk Polytechnic University, Yurga, Kemerovo oblast, 652055 Russia*
**e-mail: mrchrksv@mail.ru*

Received May 16, 2016; in final form, January 17, 2017

**Abstract**—The relaxation parameters of the lines of the *P*, *Q*, and *R* branches of the $\nu_1$ ammonia $\nu_1$ band are calculated in the case of self-broadening. In the case of doublets, the effects of collisional interference of the doublet components have been taken into account. It is shown that the cross-relaxation parameters of the components can reach ~60% of the values of the self-broadening coefficients, which gives rise to the narrowing of the components and indicates that the isolated line approximation is inapplicable. Comparison with experimental data is made. Good agreement for self-broadening coefficients is obtained. In the case of the self-shift coefficients, discrepancies are considerable in both magnitude and sign, and it is impossible to elucidate their reasons without invoking additional experimental data.

**DOI:** 10.1134/S0030400X17060054

## INTRODUCTION

The $\nu_1$ band of the ammonia molecule lies in the range of 3 μm, where it is partially overlapped with the $\nu_3$ fundamental band, with the $2\nu_4$ and $4\nu_2$ overtone bands, with the $2\nu_2 + \nu_4$ combination band, and with several hot bands. As a consequence, experimental investigations of the parameters of spectral lines of the band are fraught with considerable difficulties and theoretical calculations come to the forefront. The objectives of this work are to investigate and to calculate the relaxation parameters, which determine the contours of individual spectral lines and of the whole band, in the impact approximation. This problem is very extensive, and here we restrict ourselves to the case of self-broadening.

The $\nu_1$ vibrational–rotational band is a parallel band, but, in contrast to the $\nu_2$ band, because of a comparatively small value of the inversion splitting in the $\nu_1$ vibrational state ($\Delta\nu \sim 0.98$ cm$^{-1}$), an important role in the broadening of doublet transitions is played by processes of collisional interference of components, as this was demonstrated in [1] by the example of self-broadening of doublets of the *Q* branch of the band. A direct consequence is that the isolated line approximation cannot be applied to analyze the broadening of doublet transitions and that a special role is played by additional parameters, cross-relaxation parameters, which are responsible for the anomalous character of the pressure-induced transformation of the contours of doublets and of the entire band.

In the above-mentioned work [1], calculations were performed based on the general theory of relaxation parameters of the spectrum shape in the impact approximation [2] taking into account only one dominant dipole–dipole interaction and in the mean-velocity and rectilinear-trajectory approximations. A consistent adaptation of the theory to the case of broadening of lines of parallel and perpendicular bands of ammonia was described in [3], where the role played by the approximations mentioned above was also discussed. The material of this work will form the basis of our present investigation. We will also adhere to the notation used in that work.

Spectroscopic effects of the collisional interference of lines are frequently analyzed using the Rosenkranz theory [4]; however, this theory neither yields clear description of the physical mechanism of this phenomenon nor discusses the selection rules. This question was considered in rather great detail in [3], where it was shown, in particular, that, because rotational constant *B* of the ammonia molecule is rather large, its spectrum can be reliably modeled by a set of independently broadening singlets and doublets, but the components of doublets can be related to each other by collisional interference.

Experimental investigations of the self-broadening of lines of the $\nu_1$ band are sparse. We are aware of only the results that were described in [5, 6], in which the

self-broadening and shift coefficients of lines of the $Q$ branch with $J$ up to 9 (with some exceptions) were measured, as well as the values of these parameters for a small number of lines corresponding to $J = 0$, 1, and 3 from the $R$ branch. The authors of these works noted, in particular, that the self-broadening coefficients calculated by the Anderson–Tsao–Curnutte (ATC) method [7, 8] taking into account only one dominant dipole–dipole interaction systematically exceed the experimental values by 5–25% depending on quantum number $K$. In [1], it was shown that this fact is a consequence of the inapplicability of the isolated line approximation to the analysis of broadening of lines of the $\nu_1$ band. Because the inversion splitting of components of doublet transitions in the $\nu_1$ band is comparatively small, the collision-induced spectral exchange between the doublet components gives rise to the effect of pressure-independent narrowing of the components [1]. Taking into account this phenomenon makes it possible to construct a consistent theory and experiment.

The next section of the paper describes details of calculations, which will be performed in the rectilinear-trajectory and mean velocity approximations. Qualitatively speaking, the roles played by these approximations were discussed in [3]; however, although the applicability of the approximation of rectilinear trajectories in the case of self-broadening at room temperatures or higher is beyond question, in order to clarify the role played by the mean velocity approximation, especially in calculations of shifts of centers of lines, a more profound analysis is desirable. For this purpose, we will perform additional calculations based on a somewhat simplified model that takes into account the velocity distribution and in the mean-velocity approximation and will compare their results.

The probabilities of virtual transitions in collisional partners will be calculated in the rigid-top approximation, but the nonrigidity of molecules will be partially taken into account using the $J,K$-dependences of the average values of the dipole and quadrupole moments that are well-known from the literature. Effects related to taking into account these $J,K$-dependences will be numerically estimated.

The third section presents results of calculations and performs comparison with experimental data and with calculations implemented in the isolated line approximation. The fourth section, by the example of the $Q$ branch of the band, illustrates anomalies in the pressure-induced transformation of the spectrum shape that are caused by the collisional interference of components of doublet transitions. In particular, it is noted that one should take into account the narrowing of components upon processing an experiment with the aim of extracting information on self-broadening coefficients.

The last section briefly summarizes basic results.

## SOME COMPUTATIONAL DETAILS

As was said above, our calculations were performed based on the model that was presented in [3]. We used the rectilinear-trajectory and mean velocity approximations. Energy levels in the ground and $\nu_1$ vibrational states were calculated by the formula

$$\begin{aligned} E_\nu(J,K,\varepsilon) = E_\nu + B_\varepsilon J(J+1) + (A_\varepsilon - B_\varepsilon)K^2 \\ - D_{\varepsilon J} J^2(J+1)^2 - D_{\varepsilon JK} J(J+1)K^2 - D_{\varepsilon K} K^4 \\ + H_{\varepsilon J} J^3(J+1)^3 + H_{\varepsilon JK} J^2(J+1)^2 K^2 \\ + H_{\varepsilon JKK} J(J+1)K^4 + H_{\varepsilon KKK} K^6, \end{aligned} \quad (1)$$

where the index $\varepsilon = (a, s)$ distinguishes antisymmetric and symmetric states. The values of the spectroscopic constants are presented in Table 1.

The probabilities of virtual transitions were calculated in the rigid-top approximation, but taking into account the dependences of the average values of the dipole and quadrupole moments on rotational states in accordance with results of investigations presented in [9–11]. Thus, in [9], when studying Lamb dips in Stark spectra of $NH_3$ in the $\nu_4$ and $2\nu_2$ bands using the laser based on CO isotopes, the dependences of the average value of the dipole moment of the ammonia molecule in the ground vibrational state on the $J$ and $K$ rotational quantum numbers were modeled, and the formula was proposed

$$\begin{aligned} \mu(J,K) = 1.47182 + 1.654 \times 10^{-4} J(J+1) \\ - 3.095\times10^{-4} K^2. \end{aligned} \quad (2)$$

As follows from this formula, the dipole moment somewhat increases with increasing $J$ and decreases with increasing $K$. Thus, as $J$ increases from zero to 9 (at $K = 0$), the average value of the dipole moment increases roughly by 1%, whereas, upon an increase in $K$ from zero to 9 (at $J = 9$), it decreases approximately by 1.7%. As a consequence, this should lead to some change in the $J,K$-dependences of relaxation parameters. As for the self-broadening coefficients, this should manifest itself in a certain increase with increasing $J$ at small values of $K$ and in their decrease as $K$ approaches $J$. Unfortunately, such $J,K$-dependences for the average value of the dipole moment in the $\nu_1$ state are unavailable in the literature. In this situation, two approaches can be proposed. The first of them is based on the use of a prominent dipole moment in this state, which is calculated by the formula proposed in [10] and which is equal to 1.4792 D. The second approach uses formula (2) in which the numerical constant is equated to 1.4792. The substantiation of this approach lies in the fact that the $\nu_1$ vibration is totally symmetric with the small amplitude, and the values of the rotational constants and electrooptical parameters in this state are close to those in the ground vibrational state. We believe that this approach

**Table 1.** Spectroscopic (in units of $cm^{-1}$) and molecular parameters used in the calculation

| Parameter | $\nu_0$ [13] | | $\nu_1$ [14] | |
|---|---|---|---|---|
| | *s* | *a* | *s* | *a* |
| $\nu$ | 0 | 0.793158 | 3336.1048 | 3337.0962 |
| $B$ | 9.9465530 | 9.9415838 | 9.84868 | 9.84677 |
| $A-B$ | −3.7190265 | −3.7120883 | −3.66763 | −3.66446 |
| $D_J \times 10^4$ | 8.45775 | 8.31420 | 5.447 | 5.123 |
| $D_{JK} \times 10^4$ | −15.69125 | −15.29233 | −8.523 | −7.912 |
| $D_K \times 10^4$ | 9.082415 | 8.80628 | 4.776 | 4.802 |
| $H_J \times 10^7$ | 2.2295 | 2.04714 | 3.864 | 5.535 |
| $H_{JK} \times 10^7$ | −8.0127 | −7.25064 | −7.762 | −11864 |
| $H_{JKK} \times 10^7$ | 9.7337 | 8.66838 | 6.808 | 10.319 |
| $H_{KKK} \times 10^7$ | −3.7996 | −3.29750 | −6.228 | −6.709 |
| $M$, amu | 17.02999 | | | |
| $U$, eV | 10.16[a] | | 10.16 | |
| $\chi$, $1/cm^3$ | 2.18[b] | | 2.18 | |

Molecular parameters were taken from ([a]) [15] and ([b]) [16].

is more substantiated and will use it in the present study.

The authors of [11] have examined how the large-amplitude vibration in the ammonia molecule affects the $J,K$-dependence of the average value of the quadrupole moment. The $J$, $K$-dependence of the diagonal component was modeled by the function

$$Q_{zz}^{(\mathrm{ef})}(\nu_2; J, K) = \bar{Q}_{zz}(\nu_2) + Q_{zz}^{(J)}(\nu_2)[J(J+1) - K^2] + Q_{zz}^{(K)}(\nu_2)K^2.$$

The values of the constants were determined for symmetric ($s$) and antisymmetric ($a$) sublevels of rotational states in the ground state and in several excited vibrational states $\nu_2$. In particular, in the ground vibrational state, these constants are as follows:

$$\bar{Q}_{zz}(0) = -2.214; \quad Q_{zz}^{(J)}(0) = 0.299\times10^{-3}; \quad Q_{zz}^{(J)}(0) = -0.342\times10^{-3};\ (s)$$
$$\bar{Q}_{zz}(0) = -2.211; \quad Q_{zz}^{(J)}(0) = 0.216\times10^{-3}; \quad Q_{zz}^{(J)}(0) = -0.335\times10^{-3};\ (a).$$

Taking into account that the contribution of quadrupole interactions to the potential is comparatively small and that the values of the constants are rather close to each other, we modeled the $J,K$-dependence of the quadrupole moment of the molecule in the ground state and in the $\nu_1$ state by the function

$$q(J,K) = -2.214 + 0.299\times10^{-3}(J(J+1) - K^2) - 0.342\times10^{-3}K^2 \quad (3)$$

for both symmetric and antisymmetric states (here and below, the quadrupole moment is denoted by the symbol $q$). We note that, as distinct from the dipole moment, the magnitude of the quadrupole moment decreases with increasing $J$ (at a fixed value of $K$) and increases with increasing $K$.

The integral over the impact parameter was calculated using the procedure described in [12]. Specifically, the interval of possible values of the impact parameter was extended to 100 Å and, to take into account more exactly the nonmonotonic behavior of the integrand, was divided into three subintervals with weights 1, 2, and 3. In each subinterval, the integral was calculated by a 20-point Gauss quadrature procedure.

To estimate the roles played by the $J,K$-dependences of the average values of the dipole and quadrupole moments of the ammonia molecule and to numerically estimate errors that the mean velocity approximation introduces into the calculation, we performed additional calculations for $Q(8,K)$ lines (without dividing the interval of integration over the impact parameter into subintervals). The procedure of taking into account the velocity distribution was as follows. General formula (9) from [3], which defines the matrix elements of the relaxation operator, after factoring out the operator of averaging over relative velocities, can be represented as

$$\hat{\Lambda}_{\hat{n}\hat{m}} = -i\int_0^{+\infty} f(v)\left(\frac{\eta_b v}{c}\int_0^{+\infty} S_{\hat{n}\hat{m}}(b,v)b\,\mathrm{d}b\right)\mathrm{d}v, \quad (4)$$

**Table 2.** On the analysis of the role played by *J,K*-dependences of the average values of the dipole and quadrupole moments and of the velocity averaging in calculations of relaxation parameters (all data are expressed in units of $cm^{-1}/MPa$)

| $Q(8, K)$ | | I | | | II | | | III | | |
|---|---|---|---|---|---|---|---|---|---|---|
| $K$ | type | $\gamma$ | $\delta \times 10^2$ | $\zeta$ | $\gamma$ | $\delta \times 10^2$ | $\zeta$ | $\gamma$ | $\delta \times 10^2$ | $\zeta$ |
| 1 | *sa* | 2.354 | −1.81 | 0.201 | 2.370 | −0.75 | 0.212 | 2.341 | 0.80 | 0.203 |
| | *as* | 2.363 | 2.49 | | 2.378 | 1.97 | | 2.343 | −0.08 | |
| 2 | *sa* | 2.852 | 2.27 | 0.661 | 2.864 | 1.97 | 0.697 | 2.854 | 6.48 | 0.627 |
| | *as* | 2.860 | −1.65 | | 2.871 | −1.00 | | 2.855 | −4.72 | |
| 3 | *sa* | 3.443 | 7.45 | 1.198 | 3.445 | 5.91 | 1.261 | 3.450 | 14.25 | 1.098 |
| | *as* | 3.450 | −6.82 | | 3.451 | −5.06 | | 3.451 | −13.94 | |
| 4 | *sa* | 4.054 | 13.02 | 1.749 | 4.044 | 10.79 | 1.835 | 4.086 | 21.76 | 1.585 |
| | *as* | 4.060 | −12.32 | | 4.050 | −9.98 | | 4.087 | −21.56 | |
| 5 | *sa* | 4.691 | 18.60 | 2.303 | 4.670 | 16.23 | 2.399 | 4.748 | 29.09 | 2.074 |
| | *as* | 4.697 | −17.99 | | 4.675 | −15.62 | | 4.749 | −29.11 | |
| 6 | *sa* | 5.361 | 24.32 | 2.844 | 5.327 | 21.81 | 2.950 | 5.423 | 36.30 | 2.550 |
| | *as* | 5.365 | −24.06 | | 5.330 | −21.64 | | 5.424 | | −36.68 |
| 7 | *sa* | 6.042 | 30.79 | 3.372 | 5.977 | 26.87 | 3.538 | 6.099 | 44.20 | 3.010 |
| | *as* | 6.044 | −30.94 | | 5.978 | −27.11 | | 6.099 | −44.75 | |
| 8 | *sa* | 6.709 | 38.78 | 3.875 | 6.567 | 29.05 | 4.229 | 6.760 | 54.32 | 3.441 |
| | *as* | 6.708 | −39.43 | | 6.565 | −29.75 | | 6.760 | −54.75 | |

Calculations were performed for the $Q(8, K)$ transitions: (I) in the rigid top and mean velocity approximations, (II) in the mean velocity approximation taking into account the *J,K*-dependences of the average values of the dipole and quadrupole moments, and (III) in the rigid-top approximation taking into account the velocity distribution.

where $f(v)$ is the velocity distribution function, which, in terms of the most probable velocity, $v_m = \sqrt{\frac{2k_BT}{m}}$ ($k_B$ is the Boltzmann constant, $m$ is the reduced mass, and $T$ is the temperature), has the form

$$f(v)dv = \frac{4v^2}{\sqrt{\pi}v_m^2}\exp\left[-\left(\frac{v}{v_m}\right)^2\right]dv.$$

After introducing the new variable $y = \frac{v}{v_m}$, so that

$$f(v)\mathrm{d}v = \varphi(y)\mathrm{d}y = \frac{4y^2}{\sqrt{\pi}}\exp[-y^2]dy,$$

formula (4) takes the form

$$\hat{\Lambda}_{\hat{n}\hat{m}} = -i\frac{4\eta_b v_m}{\sqrt{\pi}c}\int_0^{+\infty}\left(\int_0^{+\infty} y^3 S_{\hat{n}\hat{m}}(b,v)\,dy\right)b\mathrm{d}b, \quad (5)$$

in which it was used in our calculations. The upper limit of the integral over velocities was assumed to be 5, since

$$\int_0^5 \frac{4y^2}{\sqrt{\pi}}\exp[-y^2]\mathrm{d}y = 0.99999999992.$$

The numerical realization was implemented using the six-point Gauss procedure.

Calculation results of described numerical estimates are presented in Table 2 along with results obtained in the rigid top and mean velocity approximations.

In the case of broadening coefficients, as was expected, taking into account the *J,K*-dependences leads to an insignificant increase in their values at small $K$ and to a roughly 2% decrease at $K$ close to 8. The effect on the shifts and cross-relaxation parameters is more considerable. The shifts decrease in magnitude, and this decrease can exceed ~30%. On the contrary, the values of the cross-relaxation parameters increase, and, at $K$ close to 8, their increase achieves ~8%.

Taking into account the distribution over relative velocities mainly leads to a small (not exceeding ~2%) increase in the values of the self-broadening coefficients, whereas the influence on the line shifts is very significant, especially at small values of $K$; however, the general character of the monotonic increase in the shift magnitudes with increasing $K$ does not change. Any more certain conclusions can be derived only if a considerable body of reliable experimental data are available.

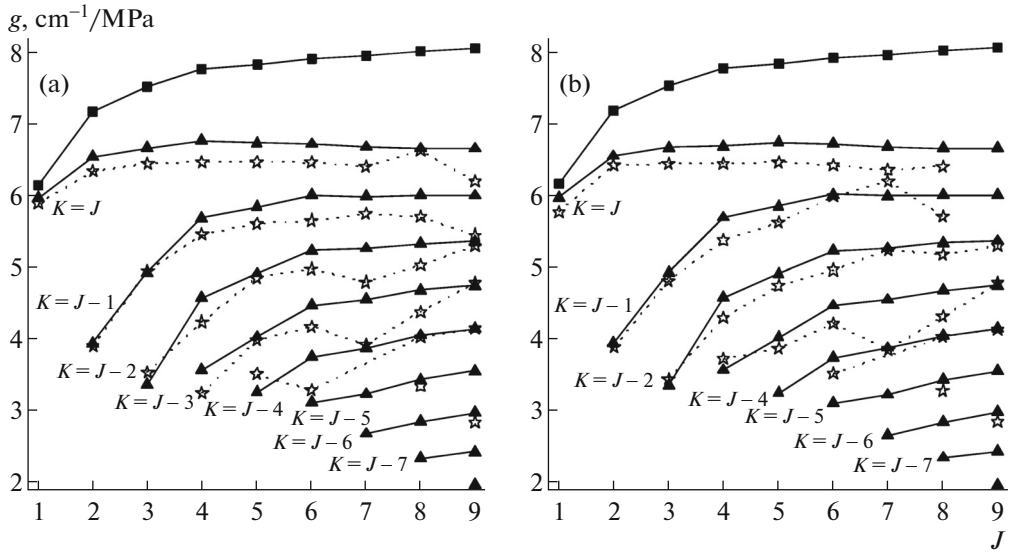


**Fig. 1.** $J$, $K$-dependences of the self-broadening coefficients of the (a) $a \leftarrow s$ and (b) $s \leftarrow a$ components of doublets of the $Q$ branch of the $\nu_1$ band at $T = 296$ K: (▲) our calculation, (☆) experimental data from [6], and (■) our calculation in the isolated line approximation for transitions with $K = J$.

## BASIC RESULTS AND COMPARISON WITH EXPERIMENT

Results of our calculations of relaxation parameters of doublet transitions are presented in Table 3. The frequencies of line centers were calculated based on formula (1) and are tentative. The character of the $J,K$-dependences of self-broadening coefficients is similar to the case of self-broadening of doublet transitions of the $\nu_2$ band [12]. However, the difference between the values of the coefficients of the $a \leftarrow s$ and $s \leftarrow a$ components is less pronounced, which is explained by a considerably smaller value of the inversion splitting of the $\nu_1$ state compared to the $\nu_2$ state. For the same reason, the values of the self-broadening coefficients of transitions of the $\nu_1$ band always exceed the values of the coefficients of the corresponding transitions of the $\nu_2$ band.

As was already noted, there is a considerable lack of experimental data on self-broadening of lines of the $\nu_1$ band of ammonia, and we are aware of only the results that were described in [5, 6]. The authors of [5] measured the self-broadening and shift coefficients of lines of the $Q$ branch and of a small number of lines of the $R$ branch. The processing was performed by the least-squares method using the Voigt contour to describe profiles of spectral lines. In [6], these same data were processed applying the global multilinear fitting procedure with the use of velocity-dependent line profile [17] modernized with allowance for the collisional interference of lines [18, 19] in terms of the Rosenkranz theory [4]. Comparison of the self-broadening coefficients of the $a \leftarrow s$ and $s \leftarrow a$ components of transitions of the $Q$ branch of the $\nu_1$ band with the experimental data from [6] is illustrated in Fig. 1. For the most part, experimental data agree satisfactorily with theoretical $J,K$-dependences. Because a similar state of affairs is also observed in the case of self-broadening of doublet transitions in the branches of the $\nu_2$ band [12], the suggestion made in this work that considerable deviations of some results from these dependences, which bear an accidental character, are consequences of experimental errors receives additional support. In Fig. 1, the $J,K$-dependences of the self-broadening coefficients of the $sQ(7, 3)$, $sQ(7, 4)$, $aQ(7, 4)$, and some other transitions refer to the results of this kind. For $Q(J, J)$ doublets, this figure also presents the results of calculations of self-broadening coefficients that were performed in the isolated line approximation. It can be seen that the anomalous exceeding of the calculation results by the ATC method [7, 8] (by 5–25% depending on the value of quantum number $K$), which was noted in [5, 6], is primarily caused by the inapplicability of the isolated line approximation.

Table 4 compares calculated shifts of line centers of the $Q$ branch with experimental data from [5, 6]. It can be seen that there is almost no agreement both in the magnitude and in the sign of shifts. For the case of lines of the $Q$ branch, the theoretical values of shifts fall on smooth curves that are shown in Fig. 2. Similar curves also take place for the $P$ and $R$ branches. However, the values of shifts determined from experiment do not fall on smooth curves. Since changes in the parameters of the intermolecular interaction within reasonable limits and, as was shown above, the aban-

**Table 3.** Relaxation parameters of the *P*, *Q*, and *R* branches of the $\nu_1$ band of the ammonia molecule at 296 K

| *P* branch | | | | | *Q* branch | | | | | *R* branch | | | | |
|---|---|---|---|---|---|---|---|---|---|---|---|---|---|---|
| Line | ν, $cm^{-1}$ | γ | $\delta \times 10^2$ | ζ | Line | ν, $cm^{-1}$ | γ | $\delta \times 10^2$ | ζ | Line | ν, $cm^{-1}$ | γ | $\delta \times 10^2$ | ζ |
| *aP*(2,1) | 3295.42 | 5.102 | −46.3 | 1.486 | *aQ*(1,1) | 3335.17 | 5.964 | −22.8 | 1.219 | *aR*(1,1) | 3374.55 | 5.095 | 13.9 | 1.493 |
| *sP*(2,1) | 3317.26 | 5.116 | −12.8 | | *sQ*(1,1) | 3336.95 | 5.964 | 21.4 | | *sR*(1,1) | 3376.33 | 5.085 | 44.3 | |
| *aP*(3,1) | 3275.24 | 3.800 | −7.93 | 1.030 | *aQ*(2,1) | 3334.81 | 3.944 | −6.90 | 1.206 | *aR*(2,1) | 3393.85 | 0.386 | −3.35 | 1.033 |
| *sP*(3,1) | 3276.96 | 3.804 | 3.54 | | *sQ*(2,1) | 3336.56 | 3.948 | 6.27 | | *sR*(2,1) | 3395.85 | 0.386 | 7.80 | |
| *aP*(3,2) | 3275.34 | 5.852 | −35.6 | 2.279 | *aQ*(2,2) | 3334.93 | 6.534 | −31.4 | 2.482 | *aR*(2,2) | 3393.99 | 5.832 | −13.1 | 2.288 |
| *sP*(3,2) | 3277.09 | 5.856 | 14.4 | | *sQ*(2,2) | 3336.72 | 6.537 | 30.9 | | *sR*(2,2) | 3395.76 | 5.831 | 34.5 | |
| *aP*(4,1) | 3254.95 | 3.664 | −3.56 | 0.660 | *aQ*(3,1) | 3334.28 | 3.361 | −1.24 | 0.821 | *aR*(3,1) | 3412.96 | 3.666 | −5.99 | 6.602 |
| *sP*(4,1) | 3256.63 | 3.676 | 4.37 | | *sQ*(3,1) | 3136.00 | 3.364 | 0.32 | | *sR*(3,1) | 3414.68 | 3.662 | 3.92 | |
| *aP*(4,2) | 3255.03 | 4.887 | −17.0 | 1.694 | *aQ*(3,2) | 3334.40 | 4.927 | −15.6 | 1.955 | *aR*(3,2) | 3413.09 | 4.885 | −13.0 | 1.694 |
| *sP*(4,2) | 3256.73 | 4.898 | 12.4 | | *sQ*(3,2) | 3336.14 | 4.929 | 14.9 | | *sR*(3,2) | 3414.83 | 4.881 | 16.9 | |
| *aP*(4,3) | 3255.18 | 6.273 | −33.6 | 2.667 | *aQ*(3,3) | 3334.61 | 6.653 | −34.6 | 2.961 | *aR*(3,3) | 3413.33 | 6.262 | −25.2 | 2.670 |
| *sP*(4,3) | 3256.92 | 6.282 | 25.5 | | *sQ*(3,3) | 3336.39 | 6.655 | 33.8 | | *sR*(3,3) | 3415.10 | 6.259 | 32.8 | |
| *aP*(5,1) | 3234.61 | 3.660 | −9.56 | 0.446 | *aQ*(4,1) | 3333.63 | 3.565 | −3.28 | 0.548 | *aR*(4,1) | 3431.92 | 3.649 | 0.6 | 0.445 |
| *sP*(5,1) | 3236.25 | 3.658 | −1.50 | | *sQ*(4,1) | 3335.31 | 3.571 | 1.85 | | *sR*(4,1) | 3433.62 | 3.650 | 8.7 | |
| *aP*(5,2) | 3234.66 | 4.491 | −16.4 | 1.261 | *aQ*(4,2) | 3333.32 | 4.567 | −11.8 | 1.466 | *aR*(4,2) | 3432.03 | 4.480 | −5.23 | 1.257 |
| *sP*(5,2) | 3236.32 | 4.490 | 4.77 | | *sQ*(4,2) | 3335.42 | 4.572 | 10.6 | | *sR*(4,2) | 3433.75 | 4.481 | 15.6 | |
| *aP*(5,3) | 3234.76 | 5.431 | −26.6 | 2.117 | *aQ*(4,3) | 3333.90 | 5.681 | −23.2 | 2.370 | *aR*(4,3) | 3432.24 | 5.419 | −13.1 | 2.111 |
| *sP*(5,3) | 3236.45 | 5.431 | 13.1 | | *sQ*(4,3) | 3335.63 | 5.684 | 22.4 | | *sR*(4,3) | 3433.98 | 5.420 | 26.0 | |
| *aP*(5,4) | 3234.95 | 6.404 | −38.3 | 2.932 | *aQ*(4,4) | 3334.19 | 6.757 | −36.7 | 3.231 | *aR*(4,4) | 3432.57 | 6.394 | −24.4 | 2.927 |
| *sP*(5,4) | 3236.67 | 6.410 | 24.5 | | *sQ*(4,4) | 3335.96 | 6.761 | 36.0 | | *sR*(4,4) | 3434.34 | 6.391 | 40.0 | |
| *aP*(6,1) | 3214.29 | 3.456 | −0.45 | 0.328 | *aQ*(5,1) | 3332.90 | 3.258 | 0.6 | 0.397 | *aR*(5,1) | 3450.80 | 3.432 | −6.07 | 0.327 |
| *sP*(6,1) | 3215.91 | 3.441 | 4.41 | | *sQ*(5,1) | 3334.57 | 3.253 | 0.96 | | *sR*(5,1) | 3452.55 | 3.437 | 0.53 | |
| *aP*(6,2) | 3214.30 | 4.105 | −7.15 | 0.986 | *aQ*(5,2) | 3332.96 | 4.032 | −5.54 | 1.137 | *aR*(5,2) | 3450.87 | 4.088 | −8.55 | 0.980 |
| *sP*(6,2) | 3215.93 | 4.096 | 7.02 | | *sQ*(5,2) | 3334.64 | 4.029 | 5.34 | | *sR*(5,2) | 3452.62 | 4.089 | 7.19 | |
| *aP*(6,3) | 3214.35 | 4.850 | −16.2 | 1.724 | *aQ*(5,3) | 3333.10 | 4.909 | −14.3 | 1.924 | *aR*(5,3) | 3451.03 | 4.838 | −12.6 | 1.712 |
| *sP*(6,3) | 3215.99 | 4.846 | 11.4 | | *sQ*(5,3) | 3334.79 | 4.908 | 13.9 | | *sR*(5,3) | 3452.77 | 4.836 | 16.3 | |
| *aP*(6,4) | 3214.45 | 5.641 | −27.8 | 2.455 | *aQ*(5,4) | 3333.33 | 5.839 | −25.0 | 2.674 | *aR*(5,4) | 3451.30 | 5.632 | −17.5 | 2.438 |
| *sP*(6,4) | 3216.11 | 5.641 | 16.7 | | *sQ*(5,4) | 3335.04 | 5.839 | 24.3 | | *sR*(5,4) | 3453.04 | 5.629 | 27.8 | |
| *aP*(6,5) | 3214.65 | 6.442 | −41.7 | 3.158 | *aQ*(5,5) | 3333.69 | 6.724 | −37.4 | 3.420 | *aR*(5,5) | 3451.72 | 6.438 | −23.6 | 3.141 |
| *sP*(6,5) | 3216.33 | 6.449 | 22.7 | | *sQ*(5,5) | 3335.43 | 6.727 | 36.1 | | *sR*(5,5) | 3453.47 | 6.432 | 41.6 | |
| *aP*(7,1) | 3194.11 | 3.150 | 3.44 | 0.265 | *aQ*(6,1) | 3332.19 | 3.121 | 0.74 | 0.309 | *aR*(6,1) | 3469.72 | 3.112 | −6.94 | 0.262 |
| *sP*(7,1) | 3195.76 | 3.118 | 6.91 | | *sQ*(6,1) | 3333.89 | 3.114 | −0.23 | | *sR*(6,1) | 3471.60 | 3.125 | −4.01 | |
| *aP*(7,2) | 3194.07 | 3.697 | −2.88 | 0.819 | *aQ*(6,2) | 3332.21 | 3.751 | −4.21 | 0.925 | *aR*(6,2) | 3469.75 | 3.670 | −8.06 | 0.807 |
| *sP*(7,2) | 3195.71 | 3.674 | 7.80 | | *sQ*(6,2) | 3333.91 | 3.746 | 4.48 | | *sR*(6,2) | 3471.60 | 3.677 | 2.55 | |
| *aP*(7,3) | 3194.03 | 4.336 | −10.7 | 1.460 | *aQ*(6,3) | 3332.28 | 4.471 | −10.7 | 1.609 | *aR*(6,3) | 3469.83 | 4.318 | −10.7 | 1.436 |
| *sP*(7,3) | 3195.67 | 4.320 | 10.3 | | *sQ*(6,3) | 3333.97 | 4.467 | 10.9 | | *sR*(6,3) | 3471.65 | 4.321 | 10.7 | |
| *aP*(7,4) | 3194.03 | 5.011 | −20.2 | 2.115 | *aQ*(6,4) | 3334.42 | 5.230 | −18.5 | 2.285 | *aR*(6,4) | 3470.01 | 5.001 | −13.8 | 2.082 |
| *sP*(7,4) | 3195.66 | 5.002 | 13.3 | | *sQ*(6,4) | 3334.11 | 5.227 | 18.4 | | *sR*(6,4) | 3471.78 | 5.001 | 20.5 | |
| *aP*(7,5) | 3194.10 | 5.713 | −31.1 | 2.749 | *aQ*(6,5) | 3332.68 | 6.005 | −27.4 | 2.928 | *aR*(6,5) | 3470.30 | 5.707 | −17.5 | 2.71 |
| *sP*(7,5) | 3195.72 | 5.709 | 16.8 | | *sQ*(6,5) | 3334.37 | 6.003 | 27.0 | | *sR*(6,5) | 3472.04 | 5.706 | 31.7 | |
| *aP*(7,6) | 3194.25 | 6.413 | −43.5 | 3.357 | *aQ*(6,6) | 3333.06 | 6.709 | −37.5 | 3.581 | *aR*(6,6) | 3470.76 | 6.412 | −22.4 | 3.323 |
| *sP*(7,6) | 3195.88 | 6.417 | 20.8 | | *sQ*(6,6) | 3334.77 | 6.711 | 36.1 | | *sR*(6,6) | 3472.48 | 6.408 | 44.1 | |

**Table 3.** (Contd.)

| *P* branch | | | | | *Q* branch | | | | | *R* branch | | | | |
|---|---|---|---|---|---|---|---|---|---|---|---|---|---|---|
| Line | ν, $cm^{-1}$ | γ | $\delta \times 10^2$ | ζ | Line | ν, $cm^{-1}$ | γ | $\delta \times 10^2$ | ζ | Line | ν, $cm^{-1}$ | γ | $\delta \times 10^2$ | ζ |
| *aP*(8,1) | 3174.21 | 2.725 | 9.57 | 0.226 | *aQ*(7,1) | 3331.64 | 2.681 | 3.51 | 0.257 | *aR*(7,1) | 3488.86 | 2.688 | −9.93 | 0.221 |
| *sP*(8,1) | 3175.98 | 2.688 | 9.70 | | *sQ*(7,1) | 3333.46 | 2.669 | −2.04 | | *sR*(7,1) | 3491.05 | 2.704 | −9.07 | |
| *aP*(8,2) | 3174.11 | 3.217 | 3.57 | 0.711 | *aQ*(7,2) | 3331.60 | 3.234 | −0.84 | 0.786 | *aR*(7,2) | 3488.82 | 3.191 | −10.9 | 0.690 |
| *sP*(8,2) | 3175.86 | 3.189 | 10.2 | | *sQ*(7,2) | 3333.41 | 3.224 | 2.12 | | *sR*(7,2) | 3490.96 | 3.201 | −2.65 | |
| *aP*(8,3) | 3173.97 | 3.797 | −3.38 | 1.277 | *aQ*(7,3) | 3331.58 | 3.876 | −6.41 | 1.387 | *aR*(7,3) | 3488.79 | 3.784 | −13.2 | 1.237 |
| *sP*(8,3) | 3175.68 | 3.777 | 12.2 | | *sQ*(7,3) | 3333.35 | 3.877 | 7.63 | | *sR*(7,3) | 3490.85 | 3.789 | 4.83 | |
| *aP*(8,4) | 3173.83 | 4.412 | −11.4 | 1.868 | *aQ*(7,4) | 3331.60 | 4.554 | −12.8 | 1.999 | *aR*(7,4) | 3488.82 | 4.409 | −15.7 | 1.809 |
| *sP*(8,4) | 3175.49 | 4.398 | 14.4 | | *sQ*(7,4) | 3333.33 | 4.548 | 13.9 | | *sR*(7,4) | 3490.78 | 4.411 | 13.3 | |
| *aP*(8,5) | 3173.73 | 5.051 | −20.9 | 2.451 | *aQ*(7,5) | 3331.72 | 5.263 | −19.9 | 2.589 | *aR*(7,5) | 3488.96 | 5.053 | −17.6 | 2.383 |
| *sP*(8,5) | 3175.35 | 5.042 | 16.2 | | *sQ*(7,5) | 3333.40 | 5.259 | 20.6 | | *sR*(7,5) | 3490.80 | 5.053 | 22.8 | |
| *aP*(8,6) | 3173.70 | 5.711 | −31.3 | 3.011 | *aQ*(7,6) | 3331.95 | 5.985 | −27.9 | 3.151 | *aR*(7,6) | 3489.23 | 5.715 | −19.8 | 2.941 |
| *sP*(8,6) | 3175.27 | 5.706 | 18.2 | | *sQ*(7,6) | 3333.60 | 5.983 | 27.7 | | *sR*(7,6) | 3490.98 | 5.713 | 33.0 | |
| *aP*(8,7) | 3173.71 | 6.378 | −43.3 | 3.538 | *aQ*(7,7) | 3332.27 | 6.667 | −37.2 | 3.715 | *aR*(7,7) | 3489.65 | 6.382 | −22.9 | 3.480 |
| *sP*(8,7) | 3175.28 | 6.380 | 20.4 | | *sQ*(7,7) | 3333.93 | 6.668 | 35.6 | | *sR*(7,7) | 3491.35 | 6.379 | 44.6 | |
| *aP*(9,1) | 3154.81 | 2.326 | 11.4 | 0.197 | *aQ*(8,1) | 3331.43 | 2.353 | 3.28 | 0.219 | *aR*(8,1) | 3508.49 | 2.288 | −9.83 | 0.188 |
| *sP*(9,1) | 3156.88 | 2.386 | 10.4 | | *sQ*(8,1) | 3333.56 | 2.343 | −2.42 | | *sR*(8,1) | 3511.26 | 2.312 | −11.3 | |
| *aP*(9,2) | 3154.63 | 2.780 | 5.46 | 0.628 | *aQ*(8,2) | 3331.33 | 2.851 | −0.86 | 0.682 | *aR*(8,2) | 3508.36 | 2.756 | −11.5 | 0.595 |
| *sP*(9,2) | 3156.65 | 2.750 | 11.1 | | *sQ*(8,2) | 3333.40 | 2.843 | 1.72 | | *sR*(8,2) | 3511.04 | 2.771 | −4.16 | |
| *aP*(9,3) | 3154.35 | 3.320 | −0.98 | 1.133 | *aQ*(8,3) | 3331.18 | 3.435 | −5.92 | 1.214 | *aR*(8,3) | 3508.19 | 3.312 | −14.5 | 1.068 |
| *sP*(9,3) | 3156.29 | 3.299 | 13.2 | | *sQ*(8,3) | 3333.18 | 3.428 | 6.92 | | *sR*(8,3) | 3510.73 | 3.321 | 3.58 | |
| *aP*(9,4) | 3154.04 | 3.891 | −7.62 | 1.666 | *aQ*(8,4) | 3331.05 | 4.049 | −11.2 | 1.767 | *aR*(8,4) | 3508.02 | 3.899 | −17.7 | 1.570 |
| *sP*(9,4) | 3155.87 | 3.875 | 15.5 | | *sQ*(8,4) | 3332.94 | 4.042 | 12.4 | | *sR*(8,4) | 3510.38 | 3.904 | 11.3 | |
| *aP*(9,5) | 3153.73 | 4.475 | −14.9 | 2.207 | *aQ*(8,5) | 3330.97 | 4.681 | −16.6 | 2.316 | *aR*(8,5) | 3507.93 | 4.497 | −19.6 | 2.090 |
| *sP*(9,5) | 3155.44 | 4.464 | 17.1 | | *sQ*(8,5) | 3332.75 | 4.675 | 17.8 | | *sR*(8,5) | 3510.07 | 4.499 | 19.0 | |
| *aP*(9,6) | 3153.45 | 5.079 | −23.0 | 2.736 | *aQ*(8,6) | 3330.98 | 5.335 | −22.4 | 2.844 | *aR*(8,6) | 3507.94 | 5.106 | −20.4 | 2.611 |
| *sP*(9,6) | 3155.05 | 5.072 | 17.8 | | *sQ*(8,6) | 3332.66 | 5.330 | 23.0 | | *sR*(8,6) | 3509.89 | 5.105 | 26.9 | |
| *aP*(9,7) | 3153.21 | 5.704 | −32.0 | 3.235 | *aQ*(8,7) | 3331.09 | 5.999 | −28.9 | 3.334 | *aR*(8,7) | 3508.09 | 5.727 | −21.5 | 3.117 |
| *sP*(9,7) | 3154.74 | 5.701 | 18.7 | | *sQ*(8,7) | 3332.70 | 5.997 | 28.7 | | *sR*(8,7) | 3509.87 | 7.725 | 35.2 | |
| *aP*(9,8) | 3152.94 | 6.350 | −42.5 | 3.678 | *aQ*(8,8) | 3331.23 | 6.645 | −37.0 | 3.815 | *aR*(8,8) | 3508.32 | 6.365 | −24.2 | 3.583 |
| *sP*(9,8) | 3154.46 | 6.352 | 20.6 | | *sQ*(8,8) | 3332.85 | 6.646 | 35.6 | | *sR*(8,8) | 3510.02 | 6.363 | 45.1 | |
| *aP*(10,1) | 3136.20 | 1.969 | 13.8 | 0.171 | *aQ*(9,1) | 3331.87 | 1.976 | 4.03 | 0189 | *aR*(9,1) | 3528.97 | 1.941 | −10.4 | 0.157 |
| *sP*(10,1) | 3138.86 | 1.931 | 11.1 | | *sQ*(9,1) | 3134.58 | 1.970 | −3.63 | | *sR*(9,1) | 3532.77 | 1.963 | −12.3 | |
| *aP*(10,2) | 3135.82 | 2.394 | 7.35 | 0.549 | *aQ*(9,2) | 3331.66 | 2.438 | −0.70 | 0.593 | *aR*(9,2) | 3528.73 | 2.390 | −13.8 | 0.450 |
| *sP*(10,2) | 3138.48 | 2.365 | 12.9 | | *sQ*(9,2) | 3334.29 | 2.432 | 1.36 | | *sR*(9,2) | 3532.38 | 2.376 | −4.11 | |
| *aP*(10,3) | 3135.48 | 2.905 | 0.31 | 0.993 | *aQ*(9,3) | 3331.36 | 2.985 | −6.30 | 1.058 | *aR*(9,3) | 3528.37 | 2.903 | −18.6 | 0.895 |
| *sP*(10,3) | 3137.89 | 2.884 | 15.9 | | *sQ*(9,3) | 3333.84 | 2.980 | 7.28 | | *sR*(9,3) | 3531.79 | 2.912 | 4.98 | |
| *aP*(10,4) | 3134.93 | 3.447 | −6.34 | 1.466 | *aQ*(9,4) | 3331.02 | 3.561 | −11.6 | 1.549 | *aR*(9,4) | 3527.95 | 3.476 | −23.2 | 1.317 |
| *sP*(10,4) | 3137.16 | 3.432 | 18.9 | | *sQ*(9,4) | 3333.31 | 3.556 | 12.9 | | *sR*(9,4) | 3531.07 | 3.472 | 13.5 | |
| *aP*(10,5) | 3134.35 | 3.996 | −12.3 | 1.958 | *aQ*(9,5) | 3330.68 | 4.147 | −16.1 | 2.053 | *aR*(9,5) | 3527.54 | 4.041 | −26.0 | 1.768 |
| *sP*(10,5) | 3136.36 | 3.985 | 20.6 | | *sQ*(9,5) | 3332.76 | 4.143 | 17.7 | | *sR*(9,5) | 3530.32 | 4.045 | 20.6 | |
| *aP*(10,6) | 3133.76 | 4.551 | −181 | 2.460 | *aQ*(9,6) | 3330.41 | 4.744 | −20.0 | 2.556 | *aR*(9,6) | 3527.20 | 4.614 | −26.4 | 2.248 |
| *sP*(10,6) | 3135.76 | 4.544 | 20.7 | | *sQ*(9,6) | 3332.28 | 4.741 | 21.5 | | *sR*(9,6) | 3529.63 | 4.616 | 26.2 | |

**Table 3.** (Contd.)

| *P* branch | | | | | *Q* branch | | | | | *R* branch | | | | |
|---|---|---|---|---|---|---|---|---|---|---|---|---|---|---|
| Line | ν, $cm^{-1}$ | γ | $\delta \times 10^2$ | ζ | Line | ν, $cm^{-1}$ | γ | $\delta \times 10^2$ | ζ | Line | ν, $cm^{-1}$ | γ | $\delta \times 10^2$ | ζ |
| *aP*(10,7) | 3133.18 | 5.122 | −24.3 | 2.947 | *aQ*(9,7) | 3330.21 | 5.360 | −24.1 | 3.039 | *aR*(9,7) | 3526.97 | 5.187 | −25.5 | 2.738 |
| *sP*(10,7) | 3134.79 | 5.118 | 20.2 | | *sQ*(9,7) | 3331.90 | 5.357 | 25.0 | | *sR*(9,7) | 3529.07 | 5.188 | 31.0 | |
| *aP*(10,8) | 3132.56 | 5.717 | −31.8 | 3.396 | *aQ*(9,8) | 3330.03 | 5.995 | −29.6 | 3.482 | *aR*(9,8) | 3526.82 | 5.767 | −25.3 | 3.209 |
| *sP*(10,8) | 3134.07 | 5.716 | 20.6 | | *aQ*(9,9) | 3331.42 | 6.650 | 36.6 | | *sR*(9,8) | 3528.68 | 5.767 | 36.7 | |
| *aP*(10,9) | 3131.77 | 6.355 | −41.8 | 3.739 | *sQ*(9.9) | 3331.64 | 5.994 | 29.6 | 3.833 | *aR*(9,9) | 3526.64 | 6.388 | −28.0 | 3.592 |
| *sP*(10,9) | 3134.07 | 6.357 | 23.1 | | *sQ*(9,8) | 3329.76 | 6.649 | −37.9 | | *sR*(9.9) | 3528.43 | 6.387 | 45.4 | |

γ is the halfwidth, δ is the shift, and ζ is the cross-relaxation parameter (all data are expressed in units of $cm^{-1}$/MPa).

donment of the mean velocity approximation can only weakly change the shape of curves presented in Fig. 2, the possibility of obtaining consistency between theory and experiment in this way loses its significance. Table 4 also presents results of calculations of shifts obtained in the isolated-line approximation, and, as one can see, this approximation, in contrast to the case of self-broadening coefficients, has only a slight effect on shifts. This is because the off-diagonal elements of matrix $\hat{A}$ are real-valued (relationship (10) from [3]). It follows from the aforesaid that, at this stage, the reasons for the discrepancy between theory and experiment with respect to shifts of line centers cannot be elucidated.

Table 5 compares calculated self-broadening and shift coefficients of lines of the *R* branch of the $\nu_1$ band with experimental data from [5, 6]. A very good agreement is observed for self-broadening coefficients. In the case of shifts of line centers, there is a certain correlation between theory and experiment both in sign and in magnitude, but quantitative discrepancies are considerable.

The self-broadening and shift coefficients of centers of singlets of the *P* and *R* branches are presented in Table 6. However, comparison with experiment is difficult because of a small number of data.

## SPECTRAL MANIFESTATIONS OF COLLISIONAL INTERFERENCE OF COMPONENTS OF DOUBLET TRANSITIONS

The numerical values of the cross-relaxation parameters, which reflects collision-induced interference of components of doublet transitions, are presented in Table 3, while their *J*,*K*-dependences are shown in Fig. 3 by the example of the *Q* branch of the band. As can be seen, the parameters decrease with increasing *J* at fixed *K* and increase with increasing *K* at fixed *J*. This character of the *J*,*K*-dependences is completely explained by the structure of the off-diag-

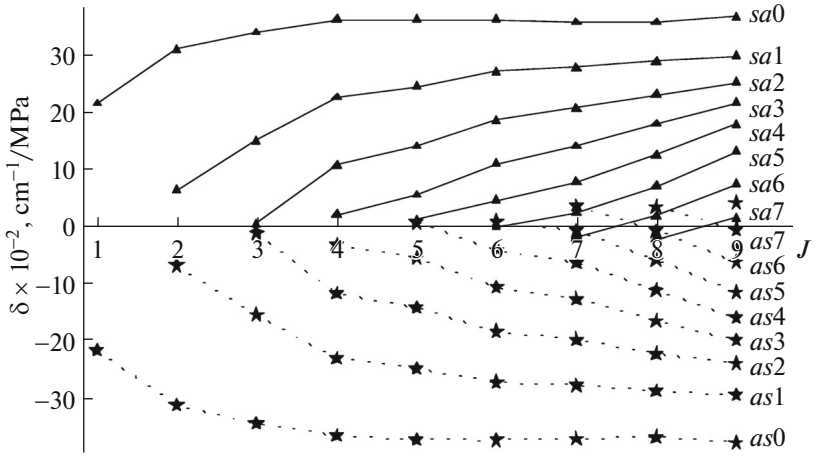


**Fig. 2.** *J*,*K*-dependences of the self-shift coefficients of the of the $s \leftarrow a$ and $a \leftarrow s$ components of doublets of the *Q* branch of the $\nu_1$ band at $T = 296$ K. Symbols *sai* and *asi* indicate curves that correspond to the $a \leftarrow s$ and $s \leftarrow a$ components with $K = J - i$.

**Table 4.** Shifts of the line centers of the $Q$ branch of the $\nu_1$ band: comparison with experiment (all data are expressed in units of $cm^{-1}$/MPa; $T = 296$ K)

| Line | $\delta \times 10^2$ | $\delta \times 10^2$ [5] | $\delta \times 10^2$ [6] | $\delta_{is} \times 10^2$ | Line | $\delta \times 10^2$ | $\delta \times 10^2$ [5] | $\delta \times 10^2$ [6] | $\delta_{is} \times 10^2$ |
|---|---|---|---|---|---|---|---|---|---|
| *aQ*(1,1) | −22.8 | −19.54 | −23.98 | −22.6 | *aQ*(6,6) | −37.5 | 3.95 | −8.0 | −36.2 |
| *sQ*(1,1) | 21.4 | 17.64 | 29.77 | 21.5 | *sQ*(6,6) | 36.1 | −5.02 | −0.3 | 36.1 |
| *aQ*(2,1) | −6.90 | −19.57 | −20.5 | −7.04 | *aQ*(7,2) | −0.84 | – | 0.0 | −1.17 |
| *sQ*(2,1) | 6.27 | −6.71 | −1.68 | 6.78 | *sQ*(7,2) | 2.12 | −68.43 | 0.0 | 2.02 |
| *aQ*(2,2) | −31.4 | −18.01 | −7.8 | −30.8 | *aQ*(7,3) | −6.41 | 1.45 | 0.0 | −6.94 |
| *sQ*(2,2) | 30.9 | 15.98 | 17.37 | 30.8 | *sQ*(7,3) | 7.63 | – | 0.0 | 7.37 |
| *aQ*(3,1) | −1.24 | −12.73 | −9.2 | −1.03 | *aQ*(7,4) | −12.8 | 18.54 | 0.0 | −13.3 |
| *sQ*(3,1) | 0.32 | −12.15 | −11.5 | 0.91 | *sQ*(7,4) | 13.9 | 12.40 | 0.0 | 13.4 |
| *aQ*(3,2) | −15.6 | −5.18 | −6.83 | −15.3 | *aQ*(7,5) | −19.9 | 0.61 | 0.0 | −20.1 |
| *sQ*(3,2) | 14.9 | −10.99 | −10.61 | 15.2 | *sQ*(7,5) | 20.6 | −8.20 | 0.0 | 20.0 |
| *aQ*(3,3) | −34.6 | −9.63 | −14.16 | −33.8 | *aQ*(7,6) | −27.9 | −7.37 | 0.0 | −27.5 |
| *sQ*(3,3) | 33.8 | 5.32 | 4.31 | 33.6 | *sQ*(7,6) | 27.7 | −4.99 | −17.92 | 27.3 |
| *aQ*(4,1) | −3.28 | 23.51 | 0.0 | −3.02 | *aQ*(7,7) | −37.2 | 2.41 | −5.54 | −35.8 |
| *sQ*(4,1) | 1.85 | 59.44 | −3.0 | 2.25 | *sQ*(7,7) | 35.6 | −13.99 | −8.23 | 35.6 |
| *aQ*(4,2) | −11.8 | 1.66 | 0.0 | −11.6 | *aQ*(8,3) | −5.92 | 24.64 | 0.0 | −6.41 |
| *sQ*(4,2) | 10.6 | 0.64 | −2.58 | 11.0 | *sQ*(8,3) | 6.92 | −39.65 | 0.0 | 6.73 |
| *aQ*(4,3) | −23.2 | −5.87 | −8.98 | −22.8 | *aQ*(8,4) | −11.2 | 12.44 | 0.0 | −11.8 |
| *sQ*(4,3) | 22.4 | −4.47 | −11.36 | 22.4 | *sQ*(8,4) | 12.4 | – | 0.0 | 12.0 |
| *aQ*(4,4) | −36.7 | −10.36 | −7.93 | −35.6 | *aQ*(8,5) | −16.6 | – | 0.0 | −17.2 |
| *sQ*(4,4) | 36.0 | 4.86 | 2.79 | 35.9 | *sQ*(8,5) | 17.8 | 19.75 | 0.0 | 17.1 |
| *aQ*(5,1) | 0.6 | 2.92 | 0.0 | 0.10 | *aQ*(8,6) | −22.4 | 4.72 | 22.98 | −22.5 |
| *sQ*(5,1) | 0.96 | 34.12 | 12.1 | −0.85 | *sQ*(8,6) | 23.0 | 0.77 | 0.0 | 22.3 |
| *aQ*(5,2) | −5.54 | −12.39 | 0.0 | −5.68 | *aQ*(8,7) | −28.9 | 9.32 | 0.0 | −28.4 |
| *sQ*(5,2) | 5.34 | −16.23 | −4.8 | 5.45 | *sQ*(8,7) | 28.7 | – | – | 28.2 |
| *aQ*(5,3) | −14.3 | −0.27 | 4.86 | −14.3 | *aQ*(8, 8) | −37.0 | −19.72 | −0.3 | −35.7 |
| *sQ*(5,3) | 13.9 | −6.83 | −5.33 | 13.9 | *sQ*(8,8) | 35.6 | – | 31.5 | 35.5 |
| *aQ*(5,4) | −25.0 | 4.46 | 0.0 | −24.5 | *aQ*(9,4) | −11.6 | 11.23 | 0.0 | −12.1 |
| *sQ*(5,4) | 24.3 | −3.23 | −9.21 | 24.2 | *sQ*(9,4) | 12.9 | −12.89 | −30.5 | 12.6 |
| *aQ*(5,5) | −37.4 | −1.06 | −13.09 | −36.1 | *aQ*(9,5) | −16.1 | −10.32 | 0.0 | −16.6 |
| *sQ*(5,5) | 36.1 | −5.98 | 2.42 | 35.9 | *sQ*(9,5) | 17.7 | – | – | 17.1 |
| *aQ*(6,2) | −4.21 | –– | 0.0 | −4.53 | *aQ*(9,6) | −20.0 | −4.01 | 0.0 | −20.4 |
| *sQ*(6,2) | 4.48 | 30.26 | 0.0 | 4.40 | *sQ*(9,6) | 21.5 | – | – | 20.7 |
| *aQ*(6,3) | −10.7 | −3.52 | – | −11.1 | *aQ*(9,7) | −24.1 | −24.17 | 0.0 | −24.2 |
| *sQ*(6,3) | 10.9 | −9.29 | −14.96 | 10.7 | *sQ*(9,7) | 25.0 | – | – | 24.3 |
| *aQ*(6,4) | −18.5 | −0.75 | 6.24 | −18.7 | *aQ*(9,8) | −29.6 | −54.16 | – | −29.2 |
| *sQ*(6,4) | 18.4 | −1.37 | −8.13 | 18.1 | *sQ*(9,8) | 29.6 | −19.87 | 5.6 | 29.1 |
| *aQ*(6,5) | −27.4 | 11.19 | 27.23 | −27.0 | *aQ*(9,9) | −37.9 | −15.91 | – | −36.6 |
| *sQ*(6,5) | 27.0 | −5.33 | −5.87 | 26.6 | *sQ*(9,9) | 36.6 | – | 16.87 | 36.4 |

$\delta$—our calculation, $\delta_{is}$—our calculation in the isolated line approximation.

**Table 5.** Self-broadening and self-shift coefficients of the lines of the $R$ branch of the $\nu_1$ band: comparison with experiment (all data are expressed in units of $cm^{-1}/MPa$; $T = 296$ K)

| Line | $\gamma$ | $\gamma_{exp}$ [5] | $\gamma_{exp}$ [6] | $\delta \times 10^2$ | $\delta_{exp} \times 10^2$ [5] | $\delta_{exp} \times 10^2$ [6] |
|---|---|---|---|---|---|---|
| $aR(1,1)$ | 5.095 | 5.162 | 5.178 | 13.9 | 2.0 | −2.48 |
| $sR(1,1)$ | 5.085 | 5.247 | 5.182 | 44.3 | 31.8 | 41.06 |
| $aR(3,1)$ | 3.666 | 3.742 | 3.743 | −5.99 | −15.3 | −14.12 |
| $sR(3,1)$ | 3.662 | 3.815 | 3.761 | 3.92 | 8.0 | 8.93 |
| $aR(3,2)$ | 4.885 | 4.969 | 4.943 | −13.0 | −17.3 | −15.68 |
| $sR(3,2)$ | 4.881 | 4.979 | 4.936 | 16.9 | 11.0 | 12.39 |
| $aR(3,3)$ | 6.262 | 6.192 | 6.210 | −25.2 | −6.36 | −6.63 |
| $sR(3,3)$ | 6.259 | 6.227 | 6.139 | 32.8 | 15.37 | 18.32 |

**Table 6.** Self-broadening and self-shift coefficients of the singlets of the $\nu_1$ band (all data are expressed in units of $cm^{-1}/MPa$; $T = 296$ K)

| $P$ branch | | | $R$ branch | | | | |
|---|---|---|---|---|---|---|---|
| Line | $\gamma$ | $\delta \times 10^2$ | Line | $\gamma$ | $\gamma_{exp}$ [6] | $\Delta \times 10^2$ | $\delta_{exp} \times 10^2$ [6] |
| $saP(1,0)$ | 3.463 | −179.2 | $asR(0,0)$ | 3.438 | 3.382 | 177.3 | 145.19 |
| $asP(2,0)$ | 2.486 | 21.87 | $saR(1,0)$ | 2.463 | 2.607 | −20.88 | 0.00 |
| $saP(3,0)$ | 2.527 | −0.95 | $asR(2,0)$ | 2.512 | | −0.34 | |
| $asP(4,0)$ | 2.960 | 2.63 | $saR(3,0)$ | 2.958 | 3.063 | −2.20 | 2.46 |
| $saP(5,0)$ | 3.211 | −4.05 | $asR(4,0)$ | 3.201 | | 2.98 | |
| $asP(6,0)$ | 3.134 | 3.13 | $saR(5,0)$ | 3.113 | | −3.05 | |
| $saP(7,0)$ | 2.852 | 7.46 | $asR(6,0)$ | 2.846 | | −7.35 | |
| $asP(8,0)$ | 2.497 | 12.68 | $saR(7,0)$ | 2.474 | | −12.34 | |
| $saP(9,0)$ | 2.076 | 10.84 | $asR(8,0)$ | 2.077 | | −9.81 | |
| | | | $saR(9,0)$ | 1.776 | | −16.10 | |

onal elements of matrix $\hat{A}$ (see (10) in [3]), which are proportional to the product of the Clebsch–Gordan coefficients $(J1K0|JK) = K/\sqrt{J(J+1)}$ for the initial and final states of the transition.

Rather large values of the parameters imply the occurrence of certain anomalies in the pressure-induced transformation of the shape of the $\nu_1$ band. In order to determine spectral manifestations of collision-induced interference of components of doublets, we performed calculations of the absorption coefficient in the frequency interval from 3331 to 3337 $cm^{-1}$, which covers the most intense lines of the $Q$ branch of the band with $J \le 8$, taking into account interference effects and using the approximation of isolated lines. The absorption coefficient was described by the formula

$$\alpha(\nu) \sim \sum_{J=1}^{8} \mu(J,K)\, \hat{R}(\nu,J,K,\varepsilon)\, \mu\rho(J,K,\varepsilon), \qquad (6)$$

where $\hat{R}(\nu,J,K,\varepsilon)$ is the resolvent of the matrix. In calculations taking into account effects of collisional interference of doublet components, this resolvent was applied in the form

$$\hat{R}(\nu,J,K,\varepsilon) = \begin{pmatrix} v - v(J,K,a) - \delta_{as}(J,K) + i\,\gamma_{as}(J,K) & i\,\zeta(J,K) \\ i\,\zeta(J,K) & v - v(J,K,s) - \delta_{sa}(J,K) + i\,\gamma_{sa}(J,K) \end{pmatrix}^{-1}, \qquad (7)$$

while, in calculations with the use of the approximation of isolated lines, it was used in the form

$$\hat{R}(\nu,J,K,\varepsilon) = \begin{pmatrix} v - v(J,K,a) - \delta_{as}(J,K) + i\,\gamma_{as}(J,K) & 0 \\ 0 & v - v(J,K,s) - \delta_{sa}(J,K) + i\,\gamma_{sa}(J,K) \end{pmatrix}^{-1}. \qquad (8)$$

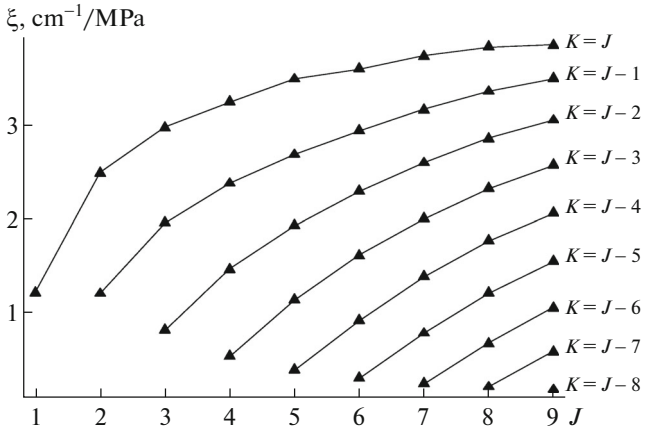


**Fig. 3.** $J$, $K$-dependences of cross-relaxation parameters of doublets of the $Q$ branch of the $\nu_1$ band at $T = 296$ K.

The intensities of lines were calculated in the rigid-top approximation, so that matrices $\mu(J,K)$ and $\mu\rho(J,K,\varepsilon)$ were applied in the form

$$\mu(J,K) = \big((J\,1\,K\,0|J\,K)\ \ (J\,1\,K\,0|J\,K)\big), \qquad (9)$$

$$\mu\rho(J,K,\varepsilon) = \begin{pmatrix} (J\,1\,K\,0|J\,K)\,\rho(J,K,1) \\ (J\,1\,K\,0|J\,K)\,\rho(J,K,-1) \end{pmatrix}. \qquad (10)$$

Here, $\rho(J,K,\varepsilon)$ is the population of the $J,K,\varepsilon$ state,

$$\rho(J,K,\varepsilon) = g(J,K,\varepsilon)\exp\{-E_0(J,K,\varepsilon)/(k_BT)\}, \quad (11)$$

where $g(J,K,\varepsilon)$ is the nuclear statistical weight of the $|J,K,\varepsilon\rangle$ state.

The calculations were performed at pressures of 10, 20, 50, and 100 Torr, and their results are presented in Fig. 4 in relative units. The plots marked by the symbol $r$ show differences between the absorption coefficients that were calculated in the isolated line approximation and taking into account collisional interference effects (residuals). Differences near centers of lines are negative, whereas, in the ranges of wings, they are positive. That is, due to the collision-induced spectral exchange between components of doublets, intensity transfer from the ranges of wings to the central parts of lines takes place. As a consequence, the line contour becomes different from the dispersion contour and its halfwidth at half-height can no longer be identified with the line halfwidth, which is customarily understood precisely as a halfwidth at half-height of the dispersion contour. However, precisely this was, in fact, done in [5, 6], and this is one of the reasons that calculated self-broadening coefficients systematically exceed experimental ones. Another reason, which, as follows from calculations and Fig. 1, is usually present, is the above-discussed effect of pressure-independent narrowing of lines due to the spectral exchange.

In order to elucidate the role played by the first of the indicated reasons, we implemented additional calculations describing the absorption coefficient of the interfering doublet by the well-known Ben–Reuven formula [20], which was represented in the form

$$\alpha(\nu) = \mathrm{Str}\,\frac{(\gamma-\zeta)\nu^2 + (\gamma+\zeta)(\Delta\nu^2 - \zeta^2 + \gamma^2)}{(\nu^2 - \Delta\nu^2 + \zeta^2 - \gamma^2)^2 + 4\gamma^2\nu^2}. \quad (12)$$

This formula was obtained for the case of two equally broadening lines with equal intensities. In the case of evaluative calculations for the $\nu_1$ band, these conditions can be considered to be met. In formula (20), $\gamma$ and $\zeta$ are theoretical parameters, which are taken from Table 3; $\Delta\nu$ is the half-spacing between the centers of the doublet components; and Str is the parameter that has the meaning of the doublet intensity, and the value of which is determined from the condition of normalization of the absorption coefficient to unity.

The calculation procedure was as follows. Doublet parameters taken from Table 3 were recalculated for the pressure of 0.05 MPa, at which the components are well separated, were substituted into (12), and coefficient Str was demonstrated from the normalization condition. Then, the maximum position, $\nu_m$, and the value of $\alpha(\nu_m)$ for the $s \leftarrow a$ doublet component were found. After that, the equation $\alpha(\nu) = 1/2\,\alpha(\nu_m)$ was solved. The self-broadening coefficient was deter-

**Table 7.** On the analysis of errors introduced into the experiment processing by neglecting the collisional interference of the doublet components

| | $aQ(1,1)$ | $aQ(2,2)$ | $aQ(3,3)$ | $aQ(4,4)$ | $aQ(5,5)$ | $aQ(6,6)$ | $aQ(7,7)$ | $aQ(8,8)$ | $aQ(9,9)$ |
|---|---|---|---|---|---|---|---|---|---|
| $\gamma_{th}$ | 5.964 | 6.534 | 6.653 | 6.757 | 6.724 | 6.709 | 6.667 | 6.645 | 6.649 |
| $\zeta_{th}$ | 1.219 | 2.482 | 2.961 | 3.231 | 3.240 | 3.581 | 3.715 | 3.815 | 3.833 |
| $\nu_{as} - \nu_{sa}$ | 1.78 | 1.78 | 1.78 | 1.77 | 1.74 | 1.71 | 1.66 | 1.62 | 1.66 |
| $\gamma_{\mathrm{mix}}$ | 5.910 | 6.399 | 6.474 | 6.558 | 6.508 | 6.478 | 6.421 | 6.389 | 6.396 |
| $\gamma_{\mathrm{exp}}$ | 5.767 | 6.415 | 6.433 | 6.434 | 6.454 | 6.411 | 6.340 | 6.396 | 6.196 |

The values of parameters $\gamma_{th}$, $\zeta_{th}$, and $\nu_{as} - \nu_{sa}$ were taken from Table 3; $\gamma_{\mathrm{exp}}$ is the experimental data from [6]; $\gamma_{\mathrm{mix}}$ is the values retrieved using the Ben–Reuven contour [20].

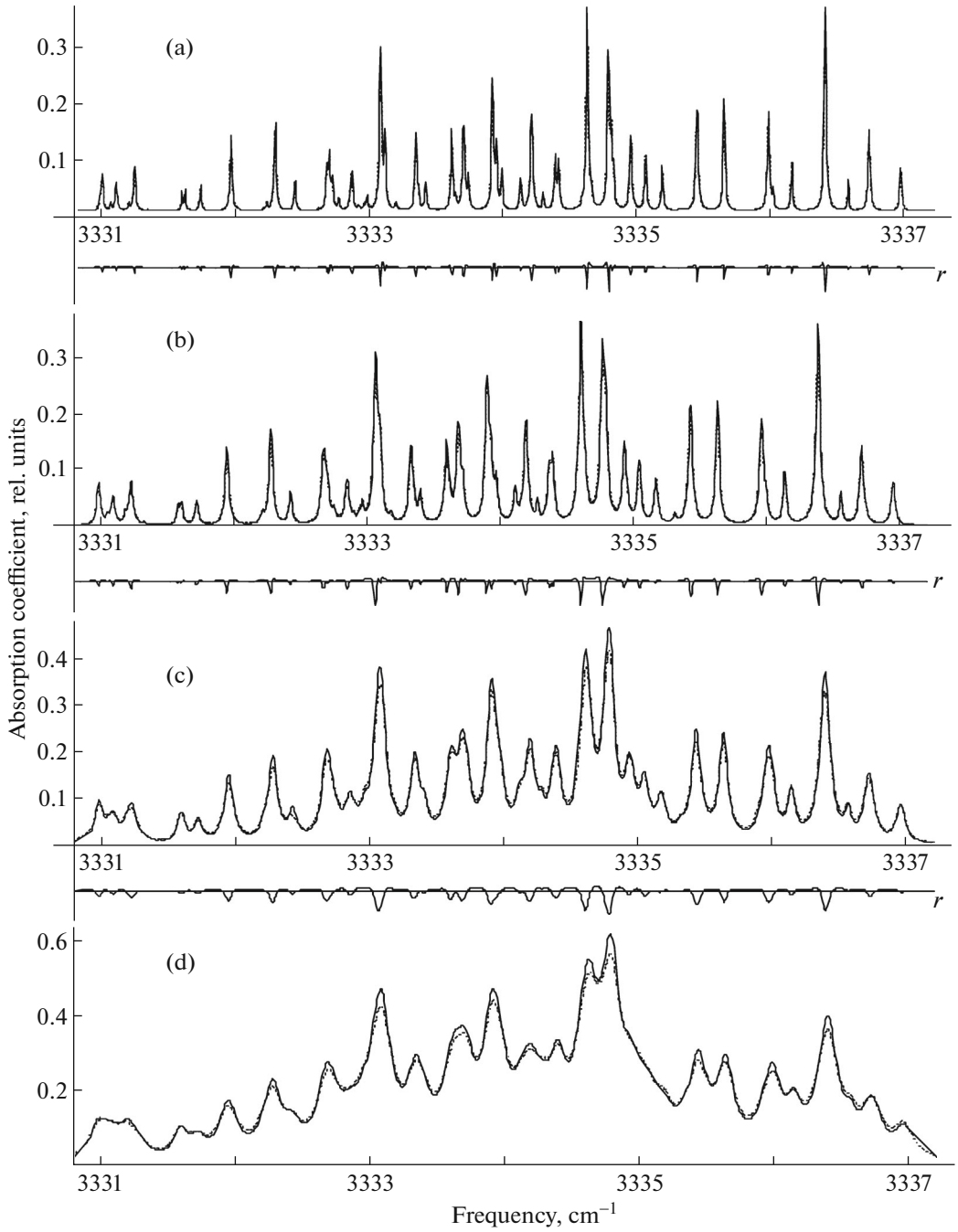


**Fig. 4.** Self-pressure induced transformations of the $Q$ branch of the $\nu_1$ band: (a) 10, (b) 20, (c) 50, and (d) 100 Torr. Solid curves refer to absorption coefficient $\alpha(\nu)$ determined taking into account spectral exchange, dashed curves refer to absorption coefficient $\alpha_{is}(\nu)$ determined in terms of the isolated line approximation, and curves marked with $r$ show differences $\alpha_{is}(\nu) - \alpha(\nu)$; $T = 296$ K.

mined as difference $\nu_m - \nu_r$, where $\nu_r$ is the root of the equation, and then was recalculated for the pressure of 1 MPa. The results of calculations of $aQ(J,J)$ ($J = 1$–9) performed for the doublet components are presented in Table 7. The first three rows contain the input parameters for calculations. Their results are presented in the fourth row, while the fifth row lists experimental data from [6]. Comparison of the first, fourth, and fifth rows of the table confirms the suggestion that the discrepancy between theory and experiment that remained after the elimination of the isolated line approximation is caused by the fact that, to extract halfwidths of doublet components from experimental absorption coefficients, the dispersion con-

tour was used rather than the Ben–Reuven contour [20], which takes into account the narrowing of contours due to the spectral exchange.

## CONCLUSIONS

The general theory of relaxation parameters of the spectrum shape in the impact approximation [1], which was adapted to the case of broadening of lines of ammonia IR spectra [3], was applied to investigate the self-broadening of lines of the $\nu_1$ band. Calculations of self-broadening and shift coefficients and cross-relaxation parameters of lines of the $P$, $Q$, and $R$ branches were performed. Comparison with experimental data from [5, 6] was made. It was proven that the systematic exceeding of self-broadening coefficients of doublet components calculated by the ATC method [7, 8] over experiment (by 5–25% depending on quantum number $K$) is caused by the inapplicability of the isolated line approximation because of the occurrence of an intense collision-induced spectral exchange between components. The abandonment of this approximation makes it possible to achieve a satisfactory agreement between calculation and experiment. A suggestion was made and confirmed by evaluative calculations that the remained discrepancy between calculated and experimental values of self-broadening coefficients is a consequence of the use of the dispersion contour for processing of measurements and neglecting the broadening of components because of the collision-induced spectral exchange.

Concerning shift coefficients, discrepancies between theory and experiment are considerable, and some correlation is observed only in the case of lines of the $R$ branch. It is impossible to make any statements about the reasons for these discrepancies without invoking reliable experimental data from other sources.

## REFERENCES

1. M. R. Cherkasov, J. Quant. Spectrosc. Radiat. Transfer **141**, 89 (2014).
2. M. R. Cherkasov, J. Quant. Spectrosc. Radiat. Transfer **141**, 73 (2014).
3. M. R. Cherkasov, Opt. Spectrosc. **120**, 827 (2016).
4. P. W. Rosenkranz, IEEE Trans. Antennas. Propag **23**, 498 (1975).
5. V. N. Markov, A. S. Pine, G. Buffa, and O. Tarrini, J. Quant. Spectrosc. Radiat. Transfer **50**, 167 (1993).
6. A. S. Pine and V. N. Markov, J. Mol. Spectrosc. **228**, 121 (2004).
7. P. W. Anderson, Phys. Rev. **76**, 647 (1949).
8. C. J. Tsao and B. Curnutte, J. Quant. Spectrosc. Radiat. Transfer **2**, 41 (1962).
9. W. H. Weber, J. Mol. Spectrosc. **107**, 405 (1984).
10. M. D. Marshal, K. S. Izgi, and J. S. Muenter, J. Chem. Phys. **107**, 1037 (1997).
11. P. Piecuch, V. Špirko, and J. Paldus, J. Chem. Phys. **105**, 11068 (1996).
12. M. R. Cherkasov, Opt. Spectrosc. **120**, 835 (2016).
13. Š. Urban, R. D'Cunha, K. N. Rao, and D. PaPoušek, Can. J. Phys. **62**, 1775 (1984).
14. R. Angstl, H. Finsterhelzl, H. Frunder, et al., J. Mol. Spectrosc. **114**, 454 (1985).
15. C.-G. Gray and K. E. Gubbins, *Theory of Molecular Fluids* (Oxford Univ. Press, London, New York, 1967).
16. R.-C. Weast, *Handbook of Chemistry and Physics,* 66th ed. (CRC, Boca Raton, FL, 1985).
17. S. G. Rautian and I. I. Sobel'man, Sov. Phys. Usp. **9**, 701 (1966).
18. R. Ciurylo, A. S. Pine, and J. Szudy, J. Quant. Spectrosc. Radiat. Transfer **68**, 257 (2001).
19. R. Ciurylo and A. S. Pine, J. Quant. Spectrosc. Radiat. Transfer **67**, 375 (2000).
20. A. Ben-Reuven, Phys. Rev. **145**, 7 (1966).

*Translated by V. Rogovoi*